Physicochem. Probl. Miner. Process., 55(2), 2019, 586-596

http://www.journalssystem.com/ppmp

Physicochemical Problems of Mineral Processing

ISSN 1643-1049

Received July 3, 2018; reviewed; accepted September 5, 2018

Molecular simulation study on hydration of low-rank coal particles and formation of hydration film

Yangchao Xia [1,2], Zili Yang [1,2], Yaowen Xing [1], Xiahui Gui [1]

[1] Chinese National Engineering Research Center of Coal Preparation and Purification, China University of Mining and Technology, Xuzhou 221116, Jiangsu, China

[2] School of Chemical Engineering and Technology, China University of Mining and Technology, Xuzhou 221116, Jiangsu, China

Corresponding author: guixiahui1985@163.com (Xiahui Gui); cumtxyw@126.com (Yaowen Xing)

Abstract: Water molecules in low-rank coal (LRC) significantly influence its upgrading and utilization. To investigate the hydration of LRC particles and the formation of a hydration film, molecular simulation techniques were innovatively used, including molecular dynamics (MD) simulations and density functional theory (DFT) calculations. The adsorption of water molecules on LRC and various oxygen-containing groups was analyzed. The results show that water molecules adsorb close to the LRC surface and form a large overlapping layer at the LRC/water interface. The radial distribution functions (RDFs) show that the adsorption affinity of water molecules on oxygen-containing sites is stronger than that on carbon-containing sites, and the RDF peaks indicate the existence of a hydration film. Moreover, the differences in adsorption between various oxygen-containing groups depend on both the number of hydrogen bonds and the adsorption distances. The calculated binding energies indicate that the adsorption capacity follows the order carboxyl > phenolic hydroxyl > alcoholic hydroxyl > ether linkage > carbonyl. Experimental results show that a high sorption rate exists between water vapor and LRC samples at the beginning of sorption, which verified the simulation results.

Keywords: Low-rank coal, water molecule, hydration film, molecular simulation

1. Introduction

Coal plays a significant role in global energy supplies and as sources of raw materials. Because of the decreasing amounts of high-grade coal, low-rank coal (LRC, including lignite and sub-bituminous coal), which accounts for approximately half of the global coal deposits, has attracted wide research attention (Sivrikaya, 2014). The high moisture content (25–70%) is a common disadvantage of LRC, which has a significant negative impact on its transportation, storage, power generation, and industrial efficiency, and can cause environmental problems (Karthikeyan et al., 2009). In view of its high water content, many drying and dewatering technologies have been continuously developed (Karthikeyan et al., 2009; Willson et al., 1997; Rao et al., 2015). The problems associate with the reduction or removal of the water content are related to the settlement of slime water and the beneficiation of fine LRC. Proper wettability is also needed to suppress coal dust (Chen et al., 2017), and reduce the occurrence of a coal seam dynamic disaster.

In order to promote the development of LRC-related industries, it is necessary to understand the coal/water interaction. Previous studies have indicated that the strong water adsorption capabilities and hydrophilic properties of LRC can be attributed to the presence of oxygenated functional groups (Chander et al., 1994; Xing et al., 2017), such as polar carboxyl, hydroxyl, and some peroxide-type oxygenated moieties. Water molecules are liable to interact with oxygen-containing groups on the coal surface, particularly with carboxyl and hydroxyl groups, via hydrogen bonds (Yu et al., 2013). Nishino indicated that carboxylic acid groups on the coal surface are the preferential adsorption sites (Nishino,

DOI: 10.5277/ppmp18170

2001). Kaji et al. reported that the water-holding capacity of coal is related to its oxygen content (Kaji et al., 1986). The interaction energy between a model coal molecule and water complexes was also investigated using DFT calculations (Gao et al., 2017; Wu et al., 2017). These studies indicate that the low-rank/oxidized coals have strong affinity for water molecules, attributed to the presence of oxygen-containing groups such as hydroxyl and carboxyl on their surfaces (Li et al., https://doi.org/10.5277/ppmp1882; You et al., https://doi.org/10.5277/ppmp18106).

Water molecules are not only easily adsorbed on the surface of hydrophilic particles but also have complex adsorption structures and specific interactions (Xu et al., 2013; Jin et al., 2014; Staszczuk, 1983; Li et al., 2015). Various researches have suggested that the surface of hydrophilic particles has a certain elastic hydration film, as confirmed via atomic force microscopy (AFM) and surface force apparatus (SFA) measurements (Butt, 1991; Pashley and Israelachvili, 1984; Pashley, 1982; Israelachvili and Mcguiggan, 1988). Recently, with the determination and establishment of the molecular structure of coal (Mathews and Chaffee, 2012; Wender, 1976), the molecular dynamics (MD) simulations have been performed to study the adsorption of water molecules on coal surface. Li et al. found that the mobility of water molecules adjacent to the hydrophilic surface becomes weaker and the molecules have a better ordering (Li, et al., 2013). You et al. found that water molecules can form an ordered layer on the surface of oxidized graphite (You et al., 2018; You et al., https://doi.org/10.5277/ppmp18106). Combines MD simulation with image processing analysis, Truong et al. investigated the structure of thin water films during the rupture process at the molecular level (Truong et al., https://doi.org/10.5277/ppmp1890). Water molecules tend to orientate toward the surface of hydrophilic minerals, such as LRC, quartz, and kaolinite, and form an ordered boundary layer called hydration film; this process is called hydration (Israelachvili, 1988; Kendall and Lower, 2004; Pashley, 1982). When two particles come into contact with each other, a repulsive hydration force is generated because of the overlap of the hydration films (Xing et al., 2018).

The existence of this hydration film affects the flocculation, settlement, and coalescence between particles, the stability of the colloid dispersion system, the removal and drying of moisture, and the adsorption of chemicals on the solid surface. No suitable instrument to measure the hydration film of coal has yet been reported so far because it is difficult to prepare a smooth solid surface meeting the test requirements, such as AFM measurement. However, molecular simulation techniques can provide information on this subject (Song and Rossky, 1994; Zhang et al., 2015; Bai et al., 2017). Herein we used molecular simulations to study the microscopic interactions of LRC/water systems and obtain a better understanding of the hydration of LRC particles and formation of hydration film. The adsorption of water molecules on both the surface and oxygen-containing groups were analysed. The investigation of hydration film is of great significance to promote the processing and utilization of hard-to-float coal.

2. Simulation details and experimental

2.1. Simulation model

In all simulated systems, the Wender coal model (lignite model) was used because its structural characteristics conform to LRC well (many side chains and oxygen atoms, but a small number of aromatic rings) (Wender, 1976). More importantly, many oxygen-containing groups (carboxyl, hydroxyl, carbonyl, and ether) were included, which is convenient to study the adsorption of water molecules. The LRC molecular structure used in the simulations is shown in Fig. 1a. In order to construct the LRC surface model, 50 coal molecules were packed into a slab (Fig. 1b).

2.2. Simulation method

Before carrying out the MD simulations, a quantum geometric optimization of the water and LRC molecule was first performed using the Materials Studio 8.0 package. The Smart method was used to optimize the LRC molecule. Then, a rectangular slab containing 50 optimized LRC molecules was built by the Amorphous Cell module. This slab was also optimized to obtain final dimensions of 40 Å × 40 Å × 33 Å and a bulk density of 1.19 g/cm^3. To model liquid water, 2000 water molecules were assembled into a slab, which was also optimized. The dimensions of the water slab were 40 Å × 40 Å × 37 Å and its

bulk density was 1.00 g/cm^3. Subsequently, the water slab was placed onto the LRC surface model to form an initial configuration (Fig. 2a).

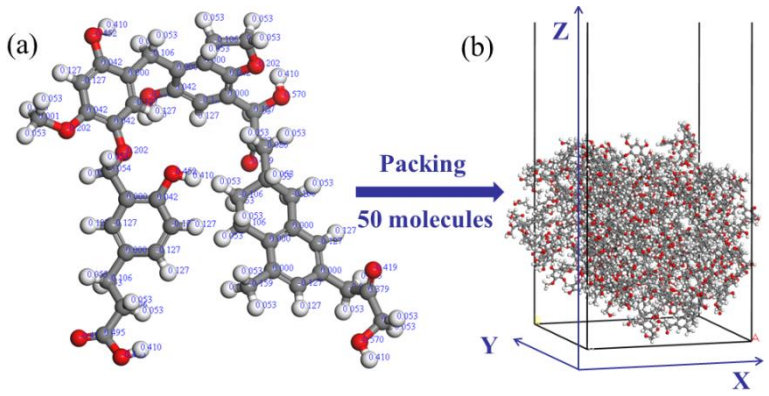

Fig. 1. LRC model (Wender, 1976): (a) molecular structure and (b) surface model. The color coding is as follows: red, white, and gray balls represent oxygen, hydrogen, and carbon atoms, respectively

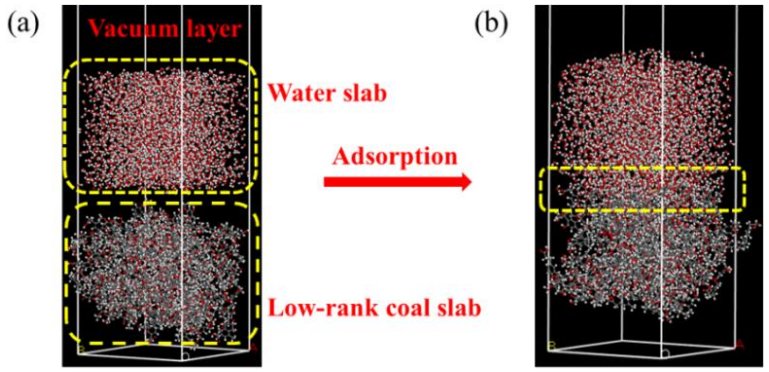

Fig. 2. Snapshots of the LRC/water adsorption process: (a) initial configuration and (b) equilibrium configuration

MD simulations were performed under periodic boundary conditions using the Forcite module. Above the model system, a vacuum layer of 100 Å in thickness was set along the Z axis. The constant-particle number, -volume and -temperature (NVT) ensemble using a Nosé thermostat was selected (Pacheco-Sánchez et al., 2003; Nosé, 1991). The temperature was maintained at 298.0 K using the Anderson thermostat. The COMPASS force field was used to simulate the atomic potential (Liu et al., 2015). The partial charges on each atom in the LRC molecule and water were calculated by the assigned force field. Fig. 1a shows the charges on the LRC atoms. The charges on the atoms in water molecule were 0.41 for H atoms and −0.82 for O atom. A time step of 1.0 fs was used to integrate the equations of motion. The Ewald method was chosen to calculate the electrostatic interaction with an accuracy of 10^{-4} kcal/mol. The atom-based method was chosen to calculate the van der Waals interactions with a cutoff of 15.5 Å. The total simulation time was 1 ns. After 500 ps, the system reached equilibrium, as shown in Fig. 3. The simulation data during the last 500 ps was used for dynamics analysis.

DFT calculations using the Dmol^3 module were performed to model the adsorption of water molecules on different oxygen-containing groups. After a single water molecule and LRC molecules were geometrically optimized, the water molecule was placed next to every oxygen-containing site on the LRC molecules. Then, a full geometry optimization of the water/oxygen-containing group system was conducted. The generalized gradient approximation (GGA) and the Perdew-Wang (PW91) exchange-correlation functional were employed in the calculations. The double-numeric quality base set with the polarization functions (DNP) was applied. A thermal smearing of 0.005 Ha and an orbital cut-off of 4 Å were used to improve the computational performance. All SCF tolerances were set to medium, i.e. the tolerances of energy, gradient, and displacement were converged to 2.0×10^{-5} Ha, 0.004 Ha/Å, and 0.005 Å, respectively.

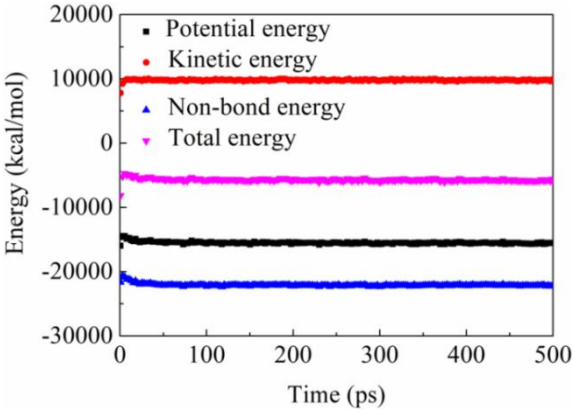

Fig. 3. Changes in energies along the simulation

2.3. Dynamic vapor sorption (DVS) measurement

The LRC samples were obtained from Shendong Mine, China. The raw samples were crushed and ground to sizes less than 200 mesh and dried in a vacuum drying oven for 24 h at 30 °C prior to use. Water sorption measurements were conducted using the Aquadyne DVS instrument (Quantachrome Ins, USA). The relative humidity was maintained at 50% by controlling the amount of water vapor. Nitrogen was used as the carrier gas and the water vapor enters the sample room with the inflow of nitrogen. The equipment automatically records the change in the quality of LRC samples over time. The experiments were repeated three times and the average value was used for calculating the moisture content as per the following equation.

$$Moisture\ content\ (\%) = \frac{m_t - m_d}{m_d} \times 100 \tag{1}$$

where m_t and m_d represent the masses of LRC samples at time t and dried LRC samples, respectively.

3. Results and discussion

3.1. Adsorption behavior of LRC/water system

Fig. 3 shows the adsorption process of the LRC/water system; the water molecules are adsorbed onto the surface and partly permeated its interior. To further understand the adsorption state, the concentration profiles of the LRC/water model system along the Z axis were calculated (Fig. 4). As observed from Fig. 4, a large overlapping region is formed, wherein the water molecules overlap with the surface in the range of 39–54 Å. These results indicate that strong interactions exist between LRC and water.

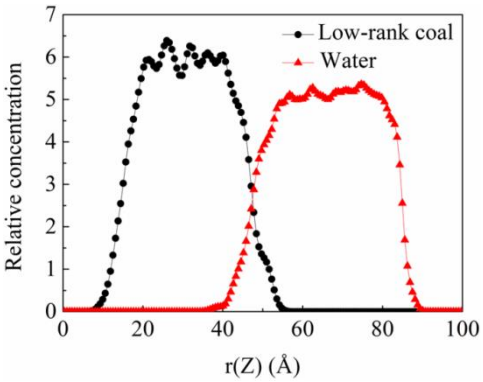

Fig. 4. Relative concentration profiles of low-rank coal and water molecules along the Z axis

Fig. 5 shows a local amplified snapshot of an adsorption equilibrium configuration. The formed hydrogen bonds can be divided into three groups: H_2O−H_2O, H_2O−LRC, and LRC−LRC. The distance-angle algorithm was used to compute the hydrogen bonds (Luzar and Chandler, 1993). In this study,

the hydrogen bonds were considered to form when the distance between hydrogen and the acceptor atom was less than 2.5 Å and the donor-hydrogen-acceptor angle was greater than 120°. Others have used a slightly different criterion in their studies. As can be seen, a large number of hydrogen bonds are formed; the numbers of hydrogen bonds for H_2O-H_2O, H_2O−LRC, and LRC−LRC were 3023, 118, and 176, respectively. The results confirm the hydrophilic characteristic of the LRC surface.

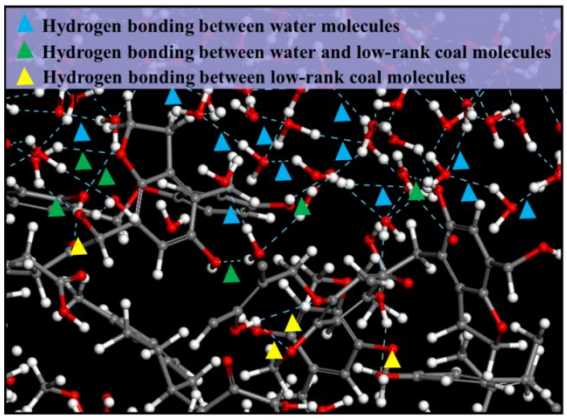

Fig. 5. Local amplified snapshot of an adsorption equilibrium configuration

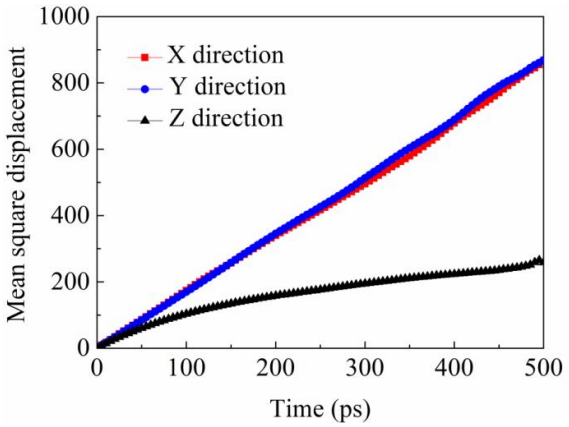

Fig. 6. Mean square displacement of water molecules along X, Y, and Z directions

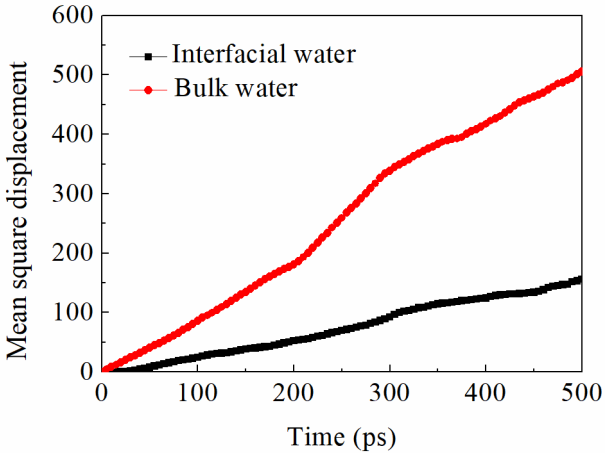

Fig. 7. Mean square displacement of interfacial and bulk water along Z direction

Hydrophilic LRC surfaces show attraction for water molecules, resulting in the movement of water molecules, which can be characterized by their diffusion coefficient (D). The diffusion coefficients were calculated as follows (Li et al., 2015):

$$MSD = \frac{1}{N}\sum_{i=1}^{N}\left[r_i(t) - r_i(0)\right]^2 \tag{2}$$

$$D = \frac{1}{6N}\lim_{t\to\infty}\frac{\mathrm{d}}{\mathrm{d}t}\sum_{i=1}^{N}\left[r_i(t) - r_i(0)\right]^2 \tag{3}$$

$$D = \lim_{t\to\infty}\left(\frac{MSD}{6t}\right) = \frac{1}{6}K_{MSD} \tag{4}$$

where *MSD* is the mean square displacement; *N* is the number of molecules; *r*(*t*) and *r*(0) are the position vectors of the center of mass of a molecule at time *t* and *t* = 0, respectively, and can be decomposed into three components (along the X, Y, and Z directions); and K_{MSD} is the slope of the linear fitting to the *MSD* vs. time curve. *D* is calculated from Eq. (4), which shows that a higher slope leads to a higher *D*. The *MSD* of water molecules along the X, Y, and Z directions are shown in Fig. 7. The result implies that the *D* values of water molecules along the X and Y directions are approximately equal and larger than that along the Z direction; this indicates that there is a lower mobility of water molecules along the Z direction. This is because the oxygen-containing groups show a strong attraction for water molecules and limit their movement. At the same time, several water molecules around the LRC surface and bulk phase were selected to compare the differences in the MSD of the interfacial water and bulk water. The results are shown in Fig. 7. According to Eq. (4), it can be inferred that *D* of interfacial water is significantly larger than that of bulk water, indicating that the dynamic characteristics of interfacial water are more stable. This may be because the interfacial water is close to the oxygen-containing groups, which have a strong adsorption capacity for water molecules.

3.2. Hydration film analysis using radial distribution functions (RDFs)

To investigate the hydration film on the LRC surface, the arrangement of water molecules around the LRC was investigated using the radial distribution function (RDF). The RDF of type B around type A molecules is calculated as follows:

$$g_{A\text{-}B}(r) = \frac{1}{4\pi\rho_B r^2}\cdot\frac{\mathrm{d}N_{A\text{-}B}}{\mathrm{d}r} \tag{5}$$

where *g*(*r*) is the value of RDF, ρ_B is the number density of type B molecules, r is the distance between A and B center of masses, and $\mathrm{d}N_{A\text{-}B}$ is the average number of type B molecules located in a region between *r* and *r*+d*r* from type A molecules. In this study, type B and type A refer to the water molecules and carbon/oxygen atoms of LRC, respectively.

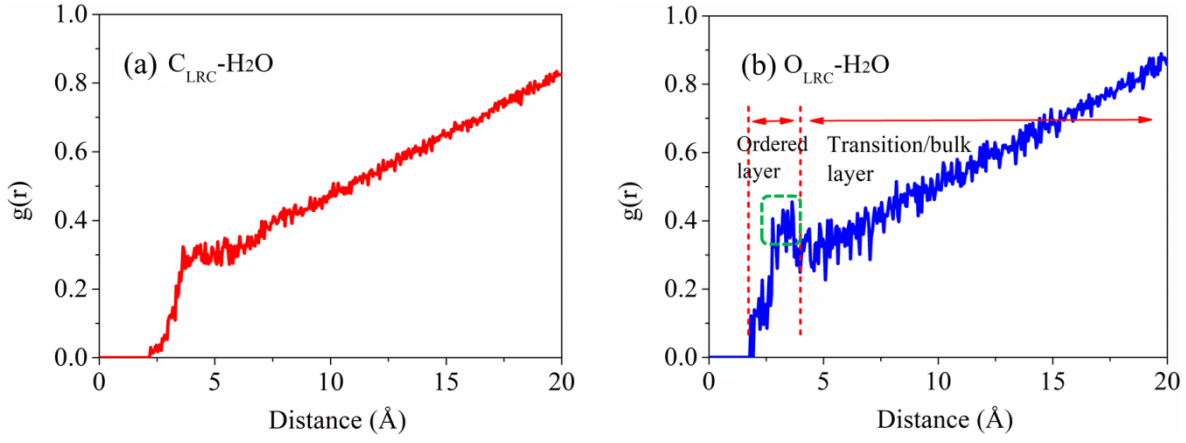

Fig. 8. Radial distribution function of water molecules around the carbon/oxygen atoms of LRC

Fig. 8(a) shows the RDF of water molecules around the carbon atoms of LRC. The adsorption distance between water molecules and carbon atoms is ~3.3 Å and no peaks appear, which indicates that the adsorption density of water molecules around the carbon-containing sites is evenly distributed and a relative weak interaction exists between water molecules and the carbon atoms of LRC. The RDF

of water molecules around the oxygen atoms of LRC is shown in Fig. 8(b). As can be seen, water molecules can be located around the oxygen atoms of LRC when the distance is ~1.9 Å. An obvious peak appears at ~2.8 Å, and then the RDF decreases to a minimum at ~3.8 Å. A comparison between both the RDFs indicates that the oxygen-containing sites have stronger affinity for water molecules, and the peak in the RDF shows that this adsorption is unevenly distributed. The density of the water phase at the peak position (2.6–3.7 Å) is higher than that in the adjacent area. Based on these results, it can be speculated that the adsorption structure of water molecules at the peak position may be regular and dense, which is different from that of bulk water. The adsorption layer of water can be divided into two regions: an ordered layer, which is defined as the hydration film, and a transition/bulk layer. It should be noted that the thickness of the hydration film may be different depending on the selected coal model and simulation method. In future, the thickness of the hydration film will be further investigated systematically by modelling a smooth coal surface, such as by adding oxygen atoms on the graphene surface.

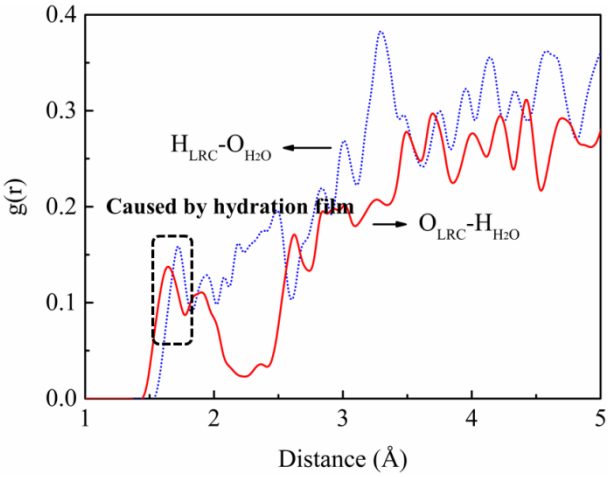

Fig. 9. Radial distribution functions of the hydrogen/oxygen atoms of water molecules around the oxygen/hydrogen atoms of LRC

To further prove the difference in the adsorption structures of water molecules in different regions, the RDFs of the hydrogen/oxygen atoms of water molecules around the oxygen/hydrogen atoms of LRC were also analyzed. As can be seen from Fig. 9, there is a distinct peak in both the RDF curves at ~1.7 Å. The peaks indicate that the adsorption structure of water molecules is compact and different from that of the adjacent area, which corresponds to the analysis of the RDFs of water molecules around the carbon/oxygen atoms of LRC. The appearance of the RDF peaks can be attributed to the formation of the hydration film. This result corresponds to the previous report (Li et al., 2018; You et al., https://doi.org/10.5277/ppmp18106). The distance of ~1.7 Å is the adsorption distance of hydrogen bonds. A detailed investigation of the hydrogen bonds between water molecules and oxygen-containing groups is presented in section 3.3.

The presence of the hydration film has an important effect on many aspects of the upgrading and utilization of LRC. In the field of LRC beneficiation, the hydration film restrains the flocculation and settlement of particles and limits the dehydration. For fine LRC particles, oily collectors, such as diesel oil and fuel oil, are commonly used as flotation collectors. However, these oily collectors cannot easily adsorb on the LRC surface owing to the obstructive effect of the hydration film, and thus affects the bubble-particle interaction and flotation performance (Staszczuk and Biliński, 1993; Xing et al., 2017). Based on the understanding of the hydration film, it is possible to find an effective solution to solve the particle-particle, particle-reagent, and particle-bubble interaction problems in various fields.

3.3. Adsorption of water molecules on various oxygen-containing groups

DFT calculations were performed to further investigate the interaction between water molecules and oxygen-containing groups. The initial configurations and Mulliken atomic charge of water molecule and oxygen-containing groups are shown in Fig. 10, and the equilibrium configurations of a single water

molecule adsorbed on carboxyl, phenolic hydroxyl, alcoholic hydroxyl, ether linkage, and carbonyl groups are given in Fig. 11. It is shown that a water molecule and an oxygen-containing group always bind through hydrogen bond. Moreover, two hydrogen bonds are observed between water and carboxyl and alcoholic hydroxyl groups. The adsorption distances between the two nearest atomic positions of a water molecule and carboxyl, phenolic hydroxyl, alcoholic hydroxyl, ether linkage, and carbonyl groups were calculated as 2.095, 1.886, 2.190, 1.988, and 2.101 Å, respectively, which agree with the previously described RDF results. The adsorption differences between these oxygen-containing groups depend on both the number of hydrogen bonds and the adsorption distances. A large number of hydrogen bonds and a short adsorption distance will together lead to a stronger adsorption. A comparison of the atomic charges in Fig. 10 and Fig. 11 revealed that the charges between water molecules and oxygen-containing groups has transferred, indicating the existence interaction between the atoms.

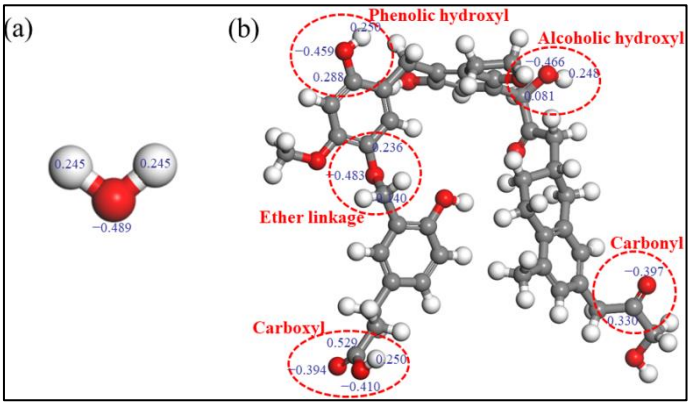

Fig. 10. Initial configuration and Mulliken charges of water molecules and oxygen-containing groups

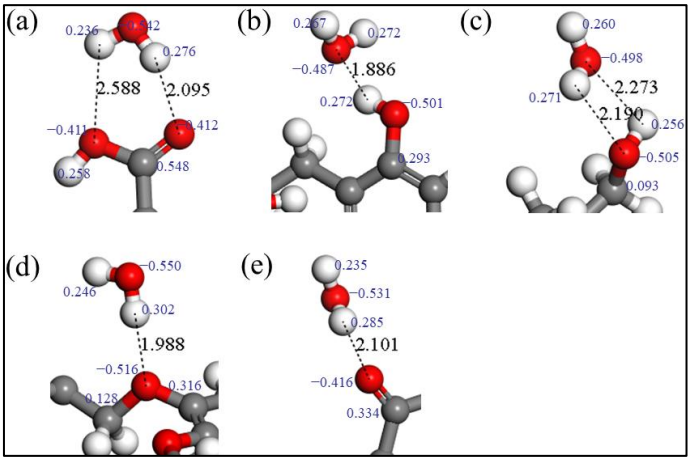

Fig. 11. Equilibrium adsorption configuration and Mulliken charges of water molecules on oxygen-containing groups: (a) carboxyl, (b) phenolic hydroxyl, (c) alcoholic hydroxyl, (d) ether linkage, and (e) carbonyl (the LRC molecules were partly presented, which can be seen in Fig. 11)

The binding energy could be directly used to identify the adsorption capacity. The binding energy between a water molecule and an oxygen-containing group of LRC is defined as follows:

$$Binding\ energy = E_{Total} - E_{Water} - E_{Oxy} \tag{6}$$

where E_{Total} is the total energy of the water/LRC system, and E_{Water} and E_{Oxy} represent the energy of a single water molecule and that of an oxygen-containing group, respectively. A more negative binding energy indicates a stronger interaction.

The binding energies calculated based on Eq. (6) are shown in Fig. 12. The negative values indicate that the adsorption process is spontaneous in all the cases. The absolute binding energy values follow the order carboxyl > phenolic hydroxyl > alcoholic hydroxyl > ether linkage > carbonyl. The binding

energy results demonstrate that carboxyl and hydroxyl groups experience a more attractive force toward a water molecule, while a weaker binding energy was calculated for the ether linkage and carbonyl groups. This is because two hydrogen bonds are formed on the carboxyl and alcoholic hydroxyl groups, and the conjugate effect of benzene causes the proton of hydrogen atoms in the −OH groups to be exposed and facilitates the formation of hydrogen bond interactions between the phenolic hydroxyl groups and the water molecules. The binding energy on the ether linkage site is higher than that on the carbonyl site, which can be attributed to the shorter adsorption distance on the ether linkage site. The DFT calculations reveal the importance of hydrogen bonds in LRC/water interaction and verify the results of the MD simulations. The hydrogen bonds between water and LRC molecules induce the high surface hydrophilic properties and result in the formation of a hydration film. These results correspond to recent studies (Gao et al., 2017; You et al., https://doi.org/10.5277/ppmp18106). It should be noted that the adsorption of water molecules on oxygen-containing groups may be different for different coal structures, but the basic trend is similarity. For example, the adsorption capacities of carboxyl and hydroxyl groups is larger than that of other oxygen-containing groups; however, the capability of carboxyl and hydroxyl groups to adsorb water molecules is not definite when these groups are present in different structures.

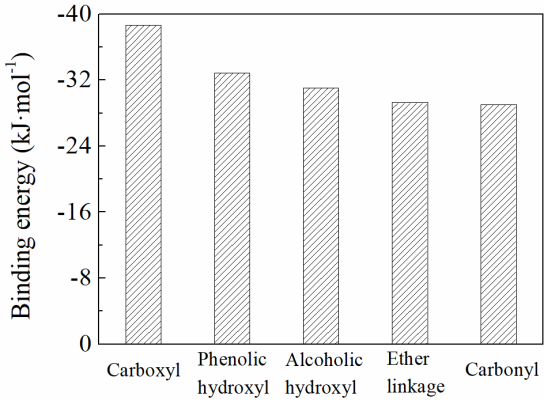

Fig. 12. Binding energy between water molecules and oxygen-containing groups

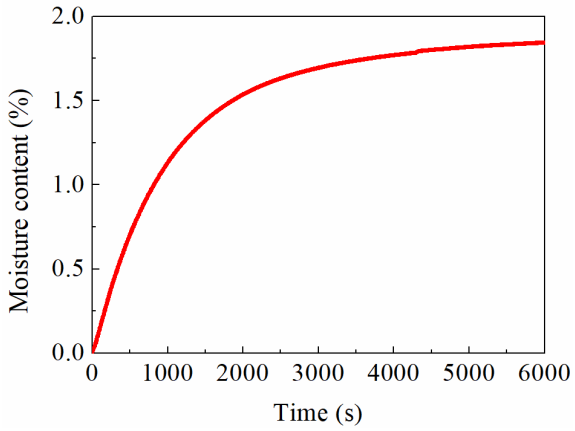

Fig. 13. Change in moisture content of LRC over time

3.4. Water vapor sorption analysis

DVS measurements were performed to investigate the sorption of water molecule by LRC. Fig. 13 shows the change in moisture content over time. It can be seen that the water content increased sharply and then slowly with an increase in time. At the beginning of sorption, the water molecules were adsorbed near the oxygen-functional groups. As the sorption progressed, the sorption rate of the water molecules become slower because these water molecules are far away from the coal surface. Hence, it can be concluded that a stronger interaction between water and LRC at the initial stages of sorption may result

from the formation of a hydration film via hydrogen bonding. The experimental results are consistent with the simulated MSD and RDF results.

4. Conclusions

Water molecules adsorbed on the surface of LRC form a large overlapping layer at the water/coal interface. A large number of hydrogen bonds are formed between water and LRC molecules. The results of MD simulations indicate that the adsorption affinity of water molecules on oxygen-containing sites is stronger than that on carbon-containing sites. The adsorption density of water molecules at the peak position is higher, probably because of the presence of a hydration film. A comparison of the MSD of interfacial water and bulk water revealed that the mobility of interfacial water was lower than that of bulk water; this implies that the water molecules near the oxygen-containing groups were adsorbed closely. Meanwhile, DVS measurements showed that the sorption rate is high at the beginning of sorption. The experimental results are consistent with the simulated MSD and RDF results.

DFT calculations indicate that water molecules are absorbed on oxygen-containing groups through hydrogen bond interaction and the adsorption conformation for each oxygen-containing group was different. The adsorption differences between these oxygen-containing groups depend on both the number of hydrogen bonds and the adsorption distances. A large number of hydrogen bonds and a short adsorption distance will lead to a stronger adsorption. The calculated binding energies show that the adsorption capacity follows the order carboxyl > phenolic hydroxyl > alcoholic hydroxyl > ether linkage > carbonyl. The investigation of the formation of hydration film is of great significance to study the LRC/water interaction involving in the processing and utilization of hard-to-float coal.

Acknowledgments

This research was supported by the National Nature Science Foundation of China (51574236, 51774286) for which the authors express their appreciation.

References

BAI, L., LI E., DU, Z., YUAN, S., 2017. *Structural changes of PMMA substrates with different electrolyte solutions: A molecular dynamics study*. Colloids Surf. A 522, 51–57.

BUTT, H.J., 1991. *Measuring electrostatic, van der Waals, and hydration forces in electrolyte solutions with an atomic force microscope*. Biophys. J. 60, 1438–1444.

CHANDER, S., POLAT, H., MOHAL, B., 1994. *Flotation and wettability of a low–rank coal in the presence of surfactants*. Miner. Metall. Process. 11, 55–61.

CHEN, Y., XU, G., ALBIJANIC, B., 2017. *Evaluation of SDBS surfactant on coal wetting performance with static methods: Preliminary laboratory tests*. Energ. Sources Part A 39, 2140–2150.

GAO, Z., DING, Y., YANG, W., HAN, W., 2017. *DFT study of water adsorption on lignite molecule surface*. J. Mol. Model. 23–27.

ISRAELACHVILI, J.N., 1988. *Forces between surfaces in liquids*. Adv. Colloid Interface Sci. 16, 31–47.

ISRAELACHVILI, J.N., MCGUIGGAN, P.M., 1988. Forces between surfaces in liquids. Sci. 241, 795–800.

JIN, J., MILLER, J.D., DANG, L.X., 2014. *Molecular dynamics simulation and analysis of interfacial water at selected sulfide mineral surfaces under anaerobic conditions*. Int. J. Miner Process. 128, 55–67.

KAJI, R., MURANAKA, Y., OTSUKA, K., HISHINUMA, Y., 1986. *Water absorption by coals: effects of pore structure and surface oxygen*. Fuel 65, 288–291.

KARTHIKEYAN, M., ZHONGHUA, W., MUJUMDAR, A.S., 2009. *Low–rank coal drying technologies–current status and new developments*. Dry. Technol. 27, 403-415.

KENDALL, T.A., LOWER, S.K., 2004. *Forces between minerals and biological surfaces in aqueous solution*. Adv. Agron. 82, 1–54.

LI, E., DU, Z., YUAN, S., CHENG F., 2015. *Low temperature molecular dynamic simulation of water structure at sylvite crystal surface in saturated solution*. Miner. Eng. 83, 53–58.

LI, E., LU, Y., CHENG, F., WANG, X., MILLER, J. D. *Effect of oxidation on the wetting of coal surfaces by water: experimental and molecular dynamics simulation studies*, Physicochem. Probl. Miner. Process. http://dx.doi.org/10.5277/ppmp1882.

LI, E.Z., DU, Z.P., YUAN, S.L., 2013. *Properties of a water layer on hydrophilic and hydrophobic self–assembled monolayer surfaces: A molecular dynamics study*. Sci. China Chem. 56, 773–781.

LIU, A., FAN, J., FAN, M., 2015. *Quantum chemical calculations and molecular dynamics simulations of amine collector adsorption on quartz (0 0 1) surface in the aqueous solution*. Int. J. Min. Process. 134, 1-10.

LUZAR, A., CHANDLER, D., 1993. *Structure and hydrogen bond dynamics of water–dimethyl sulfoxide mixtures by computer simulations*. J. Chem. Phys. 98, 8160–8173.

MATHEWS, J.P., CHAFFEE, A.L. 2012. *The molecular representations of coal–A review*. Fuel 96, 1–14.

NISHINO, J., 2001. *Adsorption of water vapor and carbon dioxide at carboxylic functional groups on the surface of coal.* Fuel 80, 757–764.

NOSÉ, S., 1991. *Constant temperature molecular dynamics methods*. Prog. Theor. Phys. Supp. 103, 1-46.

PACHECO-SÁNCHEZ, J.H., ZARAGOZA, I.P., MARTÍNEZ-MAGADÁN, J.M., 2003. *Asphaltene aggregation under vacuum at different temperatures by molecular dynamics*. Energy Fuels 17, 1346-1355.

PASHLEY, R.M., 1982. *Hydration forces between mica surfaces in electrolyte solutions.* Adv. Colloid Interface Sci. 16, 57–62.

PASHLEY, R.M., ISRAELACHVILI, J.N., 1984. *Molecular layering of water in thin films between mica surfaces and its relation to hydration forces.* J. Colloid Interface Sci. 101, 511–523.

RAO, Z., ZHAO, Y., HUANG, C., DUAN, C., HE, J., 2015. *Recent developments in drying and dewatering for low rank coals*. Prog. Energ. Combust. 46, 1–11.

SIVRIKAYA, O., 2014. *Cleaning study of a low-rank lignite with DMS, Reichert spiral and flotation*. Fuel 119, 252–258.

SONG, H.L., ROSSKY, P.J., 1994. *A comparison of the structure and dynamics of liquid water at hydrophobic and hydrophilic surfaces–a molecular dynamics simulation study*. J. Chem. Phys. 100, 3334–3345.

STASZCZUK, P., 1983. *Effect of flotation reagents on hydration of pit-coal and limestone surfaces part I. Investigations of hydration layers on the surface of minerals and the role of diesel oil in the pit-coal cleaning process*. Powder Technol. 34, 161-165.

STASZCZUK, P., BILIŃSKI, B., 1993. *Water film properties on mineral surfaces in flotation processes*. Colloids Surf. A 79, 97–104.

TRUONG, V.N.T., DANG, L.X., LIN C.-L., WANG. X., MILLER, J.D. *Water film structure during rupture as revealed by MDS image analysis.* Physicochem. Probl. Miner. Process. https://doi.org/10.5277/ppmp1890.

WENDER, I., 1976. *Catalytic synthesis of chemicals from coal*. Catal. Rev. 14, 97–129.

WILLSON, W.G., DAN, W., IRWINC, W., 1997. *Overview of low-rank coal (LRC) drying*. Coal Prep. 18, 1–15.

WU, J., WANG, J., LIU, J., YANG, Y., CHENG, J., WANG, Z., ZHOU, J., CEN, K., 2017. *Moisture removal mechanism of low–rank coal by hydrothermal dewatering: Physicochemical property analysis and DFT calculation*. Fuel 187, 242–249.

XING, Y., GUI, X., CAO, Y., 2018. *Hydration film measurement on mica and coal surfaces using atomic force microscopy and interfacial interactions*. J. Cent. South Univ. 25, 1295−1305.

XING, Y., GUI, X., PAN, L., PINCHASIK, B.E., CAO, Y., LIU, J., KAPPL, M., BUTT, H.J., 2017a. *Recent experimental advances for understanding bubble–particle attachment in flotation*. Adv. Colloid Interface Sci. 246, 105–132.

XING, Y., LI, C., GUI, X., CAO, Y., 2017b. *Interaction forces between paraffin/stearic acid and fresh/oxidized coal particles measured by atomic force microscopy*. Energy Fuels 31, 3305–3312.

XU, Y., LIU, Y.L., HE, D.D., LIU, G.S., 2013. *Adsorption of cationic collectors and water on muscovite (001) surface: A molecular dynamics simulation study*. Miner. Eng. 53, 101–107.

YOU, X., HE M., CAO, X., LYU, X., LI L. *Structure and dynamics of water adsorbed on the lignite surface: Molecular dynamics simulation.* Physicochem. Probl. Miner. Process. https://doi.org/10.5277/ppmp18106.

YOU, X., WEI, H., ZHU, X., LYU, X., LI, L., 2018. *Role of oxygen functional groups for structure and dynamics of interfacial water on low rank coal surface: a molecular dynamics simulation*. Mol. Phys. 116, 1670–1676.

YU, J., TAHMASEBI, A., HAN, Y., YIN, F., LI, X., 2013. *A review on water in low rank coals: The existence, interaction with coal structure and effects on coal utilization*. Fuel Process. Technol. 106, 9–20.

ZHANG, Z., WANG, C., YAN, K., 2015. *Adsorption of collectors on model surface of Wiser bituminous coal: A molecular dynamics simulation study*. Miner. Eng. 79, 31–39.